Materials Letters 124 (2014) 261–263

Contents lists available at ScienceDirect

Materials Letters

journal homepage: www.elsevier.com/locate/matlet

Formation of Sn-rich phases via the decomposition of Cu_6Sn_5 compounds during current stressing

C.K. Lin, Chien-Ming Liu, Chih Chen *

Department of Materials Science and Engineering, National Chiao Tung University, Hsin-chu 30010, Taiwan, ROC

ARTICLE INFO

Article history:
Received 5 March 2014
Accepted 13 March 2014
Available online 21 March 2014

Keywords:
Phase transformation
Metallic composites
Intermetallic compound
Solder
Electromigration

ABSTRACT

This study examined the formation of Sn-rich phases in the matrix of Cu–Sn–Ni intermetallic compounds (IMCs) after current stressing of 1.2×10^4 A/cm^2 at 160 °C. The Sn-rich phases were formed at the cathode end of the solder joints with Cu metallization, and this formation was attributed to the decomposition of Cu_6Sn_5 IMCs. When the Cu_6Sn_5 IMCs were transformed into Cu_3Sn during current stressing, Sn atoms were released. When the supply of Cu atoms became deficient, Sn atoms accumulated to form Sn-rich phases among the Cu–Sn–Ni IMCs.

1. Introduction

Electromigration has been one of the most persistent reliability issues in microelectronic devices [1–3]. As the dimensions of devices continue to shrink, solder joints must be reduced in size accordingly. In addition, with higher performance required of devices, the operating current in each solder joint increases progressively, leading to a dramatic increase in the current density in the joint. Therefore, electromigration has become a critical reliability issue [4,5].

Many efforts have been devoted to understanding electromigration behavior [6–12]. Electromigration may induce void formation in solder [13–15]. In addition, electron flow may enhance the dissolution of under bump metallization (UBM) and cause the extensive formation of intermetallic compounds (IMCs) [16–20]. Both mechanisms can lead to an open circuit of solder joints.

Pb-free solders have been adopted to replace Pb-containing solders [21,22]. Compared with Pb-containing solder, Pb-free solders possess higher reaction rates with Cu and Ni UBMs [7,17,23,24]. Therefore, extensive Cu–Sn IMCs are formed during electromigration in Pb-free solders with Cu UBMs [9,10]. Both Cu_3Sn and Cu_6Sn_5 IMCs are formed after current stressing. In addition to these two IMCs, Sn-rich phases have also been frequently observed at the cathode end [10,25,26]. However, the reason for the formation of Sn-rich phases among the Cu–Sn IMCs after electromigration remains unclear.

This study investigated electromigration in Pb-free SnAg solder joints containing Cu/Ni UBMs. Sn-rich phases were formed after current stressing of 1.2×10^4 A/cm^2 at 150 °C. A mechanism was proposed to explain this interesting phenomenon.

2. Experimental

Sample dimensions and test conditions: Flip-chip Sn-2.3Ag (wt%) solder joints were used for the electromigration tests. Fig. 1(a) presents a schematic structure for the test layout. Currents were applied at Nodes N2 and N3. The voltage was measured at Nodes N1 and N4. Fig. 1(b) presents a schematic drawing of the joint and Fig. 2(a) presents a cross-sectional SEM image of the joint. The thickness of the Cu traces on the chip side was 5 μm, whereas the thickness was 20 μm on the FR-5 substrate side. The 500-Å-thick Ti seed layer was between the Cu trace and the Cu UBM. The UBM on the chip side comprised electroplated 5-μm Cu and 3-μm Ni. On the substrate side, the metallization was electroless Ni. For the as-fabricated sample, the interfacial IMCs were Ni_3Sn_4 on both the chip and substrate sides. Kelvin bump structures were employed to measure the individual bump resistance [15]. The solder joints were stressed at a current density of 1.2×10^4 A/cm^2 at 150 °C. The actual stressing temperature was calibrated using the temperature coefficient of resistivity of the Cu trace on the chip side [27]. The actual stressing temperature increased to 160 °C due to the Joule heating effect in the solder joints [28].

Analytical procedures: As the resistance reached a desired value, the current stressing was terminated, and the sample was polished for cross-sectional observation using a JEOL 6700 scanning electron microscope (SEM). Energy dispersive spectrometry (EDS) was

* Corresponding author. Tel.: +886 3 5731814; fax: +886 3 5724727.
E-mail addresses: chih@mail.nctu.edu.tw, chihchen98@yahoo.com (C. Chen).

http://dx.doi.org/10.1016/j.matlet.2014.03.071
0167-577X/

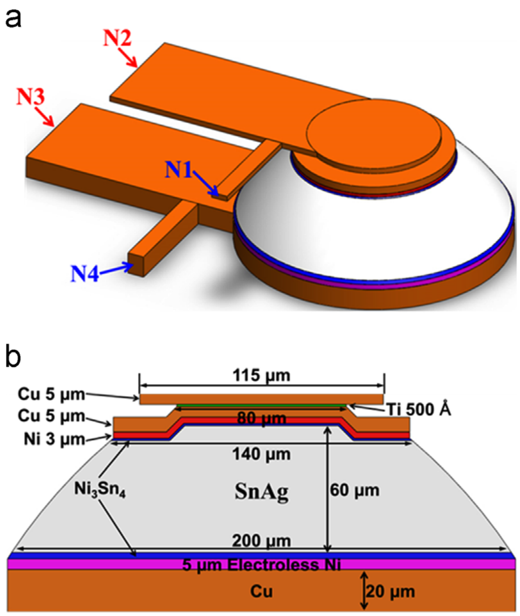

Fig. 1. (a) Layout for electromigration tests and four-point structure for measuring bump resistance. (b) Schematic diagrams of the solder joints investigated in this study.

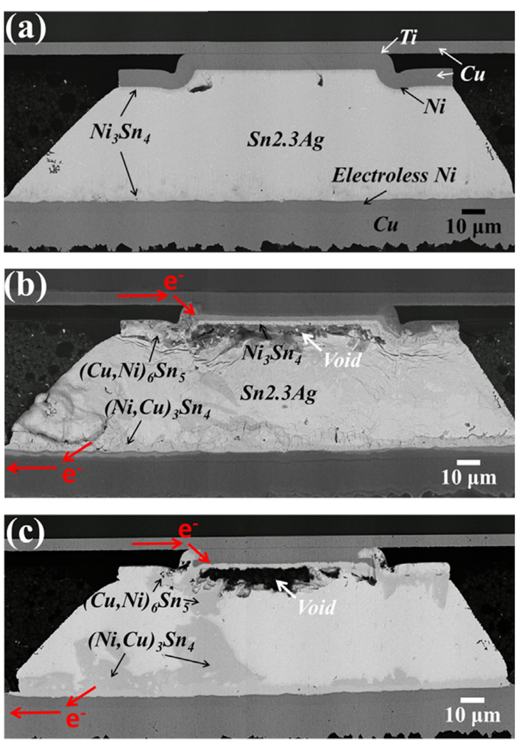

Fig. 2. (a) Cross-sectional SEM image of the Sn2.3Ag solder bump before current stressing. The electrons entered from the upper-left corner and exited from the lower-left corner. (b) Cross-sectional SEM image showing the microstructure of the solder joint after current stressing of 1.2×10^4 A/cm^2 at 160 °C for 678 h. (c) Microstructure of the joint in Fig. 2(b) after slight polishing.

employed to analyze the composition of the solder joint and IMCs. A focused ion beam (FIB) was utilized to prepare the samples for observation using an ion image.

3. Results

Electromigration-enhanced growth of IMCs occurred before the formation of the Sn-rich phases. Fig. 2(b) displays a cross-sectional SEM image of the solder joint stressed with a downward electron flow for 678 h. The resistance of the joint increased by 25% of its original value. Several voids were observed below the passivation opening. In addition, four types of IMCs were detected on the chip side, including $(Ni,Cu)_3Sn_4$, Cu_6Sn_5, Cu_3Sn, and $(Cu,Ni)_6Sn_5$. The positions of the IMCs are labeled in the figure. The formation of Cu–Sn and Cu–Sn–Ni IMCs was attributed to the migration of the Cu UBM into the solder after the 3-µm Ni was consumed. Current crowding was significant in the upper-left corner [29]. Hence, the Ni layer there dissolved faster than in other locations.

To more clearly examine the microstructure of the joint, the joint was polished slightly to remove the rough surface due to current stressing. Fig. 2(c) shows the microstructure of the joint in Fig. 2(b) after slight polishing, and Fig. 3(a) is an enlarged SEM image of the upper-left corner. It is interesting that the Sn-rich region was observed among the IMCs, as indicated by one of the arrows in Fig. 3(a). The SEM/EDS analysis revealed that the composition of the Sn-rich phases was 100% Sn. The Sn-rich phases were usually located close to the cathode end near the current-crowding region and were surrounded by Cu–Ni–Sn IMCs. Note that the Cu UBM above the Sn-rich region was completely consumed.

To further analyze the Sn-rich phases, FIB was employed to cut a second cross-sectional sample from the region. The location of the sample is indicated by the white dashed line in Fig. 3(a). Fig. 3(b) displays the FIB ion image of the location after FIB etching. A Sn-rich region with a width of approximately 5 µm was observed, as indicated by the arrows. This region was surrounded by Cu–Sn–Ni IMCs. The volume of this region was estimated to be 30 µm^3. Located below the Pt layer and surrounded by Cu–Sn–Ni IMCs, these Sn-rich phases melted.

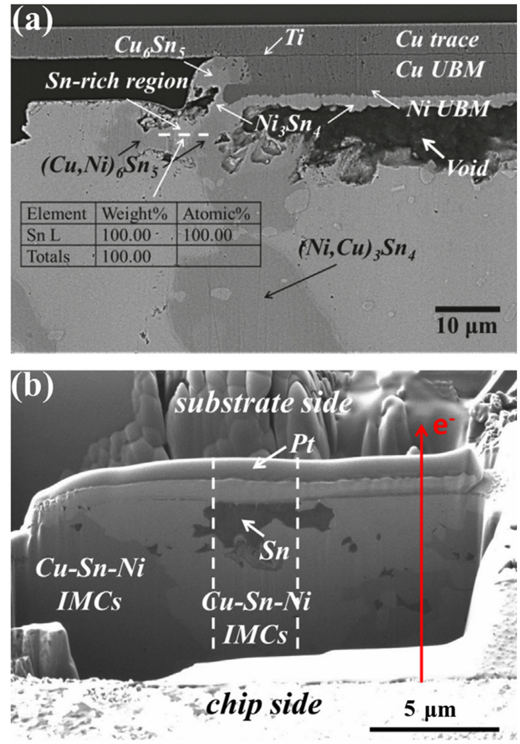

Fig. 3. (a) Enlarged SEM image of the upper-left corner. (b) Analysis of the Sn-rich region by FIB. The ion image showing a Sn-rich region of approximately 5 µm wide surrounded by Cu–Sn IMCs after FIB etching.

4. Discussion

Phase transformation of IMCs was proposed as the main mechanism for the formation of Sn-rich phases in the IMC region.

When the Cu UBM on the chip side was dissolved due to the downward electron flow, the interfacial Ni_3Sn_4 IMCs were converted into $(Cu,Ni)_6Sn_5$. In addition, when the Cu_6Sn_5 IMCs were annealed at 160 °C, some of the Cu_6Sn_5 IMCs were transformed into Cu_3Sn [30]:

$$Cu_6Sn_5 \rightarrow 2Cu_3Sn + 3Sn. \quad (1)$$

The pure Sn released from this phase transformation may have reacted with the incoming Cu flux to form Cu–Sn IMCs. However, when the Cu flux became deficient, the Sn-rich phase was formed in the Cu–Sn IMC region. A deficiency of Cu may have been present in the upper-left corner due to the following two reasons. First, Cu atoms continuously migrated to the substrate side due to the electron wind force, and Cu was quite susceptible to diffuse in the solder under electromigration [1]. Second, the thickness of the Cu UBM was only 5 μm. After the Cu UBM was completely dissolved into the solder by the electron wind force, the supply of Cu atoms was not sufficient to maintain the Cu–Sn IMCs on the chip side, resulting in the formation of Sn-rich phases in the current-crowding region at the cathode end.

In solid-state metallurgical reactions without current stressing, there have been no reports on Sn-rich phase formation due to the decomposition of Cu_6Sn_5 IMCs into Cu_3Sn because when the three excess Sn atoms are released, they will react with nine Cu atoms to form Cu_3Sn [30]. In general, the supply of Cu is not an issue for metallurgical reactions. Therefore, the formation of the Sn-rich phase due to the decomposition of Cu_6Sn_5 IMCs has never been reported.

5. Conclusions

In summary, an interesting phenomenon of Sn-rich phase formation was observed after current stressing of 1.2×10^4 A/cm^2 at 160 °C in SnAg solder joints. Sn-rich phases were formed among the IMCs at the cathode end. The decomposition of Cu_6Sn_5 into Cu_3Sn IMCs may have caused the Sn-rich phase formation. Phase transformation results in the release of Sn atoms, which accumulate into the Sn-rich phases, where the incoming Cu flux becomes deficient.

Acknowledgments

The authors gratefully acknowledge the financial support of the National Science Council of the Republic of China (Grant No. NSC 99-2221-E-009-040-MY3).

References

[1] Chen C, Tong HM, Tu KN. Annu Rev Mater Sci 2010;40:531–55.
[2] Tu KN. J Appl Phys 2003;94:5451–73.
[3] Chan YC, So ACK, Lai JKL. Mater Sci Eng B 1998;55:5–13.
[4] Liu CY, Chen C, Liao CN, Tu KN. Appl Phys Lett 1999;75:58–60.
[5] Brandenburg S, Yeh S. Proceedings of surface mount international conference and exhibition, San Jose; 1998. p. 337–344.
[6] Chen CM, Chen SW. J Electron Mater 1999;28:902–6.
[7] Lee TY, Choi WJ, Tu KN, Jang JW, Kuo SM, Lin JK, et al. J Mater Res 2002;17:291–301.
[8] Zeng K, Stierman R, Chiu TC, Edwards D, Ano K, Tu KN. J Appl Phys 2005024508-1–8.
[9] Ding M, Wang G, Chao B, Ho PS, Su P, Uehling T. J Appl Phys 2006094906-1–6.
[10] Lin YH, Tsai CM, Hu YC, Lin YL, Kao CR. J Electron Mater 2005;34:27–33.
[11] Lin CT, Chuang YC, Wang SJ, Liu CY. Appl Phys Lett 2006101906-1–3.
[12] Liu YH, Lin KL. J Mater Res 2005;20:2184–93.
[13] Yeh ECC, Chos WJ, Tu KN, Elenius P, Balkan H. Appl Phys Lett 2002;80:580–2.
[14] Shao TL, Chen YH, Chiu SH, Chen C. J Appl Phys 2004;96:4518–24.
[15] Chang YW, Chiang TH, Chen C. Appl Phys Lett 2007;91:132113-1-132113-3.
[16] Hu YC, Lin YH, Kao CR, Tu KN. J Mater Res 2003;18:2544–8.
[17] Zeng K, Stierman R, Chiu TC, Edwards D, Ano K, Tu KN. J Appl Phys 2005;97:024508–1-024508-8.
[18] Chae SH, Zhang X, Lu KH, Chao HL, Ho PS, Ding M, et al. J Mater Sci Mater El 2007;18:247–58.
[19] Liang YC, Tsao WA, Chen C, Yao DJ, Huang AT, Lai YS. J Appl Phys 2012043705-1–043705-7.
[20] Chen HY, Ku MF, Chen C. Adv Mater Res 2012;1:83–92.
[21] Yazzie KE, Fei H, Jiang H, Chawla N. Acta Mater 2012;60:4336–48.
[22] Zeng K, Tu KN. Mat Sci Eng R 2002;38:55–105.
[23] Bath J. Lead-free soldering. Springer; 2007; 39.
[24] Subramanian KN. Lead-free electronic solders. Springer; 2007; 21.
[25] Ke JH, Chuang HY, Shih WL, Kao CR. Acta Mater 2012;60:2082–90.
[26] Lin YW, Ke JH, Chuang HY, Lai YS, Kao CR. J Appl Phys 2010;107:073516–1-073516-4.
[27] Chen HY, Chen C. J Mater Res 2010;25:1847–53.
[28] Chiu SH, Shao TL, Chen C, Yao DJ, Hsu CY. Appl Phys Lett 2006022110-1–3.
[29] Liang SW, Chang YW, Chen C, Liu YC, Chen KH, Lin SH. J Electron Mater 2006;35:1647–54.
[30] Tu KN. Solder joint technology: materials properties, and reliability. New York: Springer; 2007.